

Atomistic Study of Dislocation Loop Emission from a Crack Tip

Ting Zhu,¹ Ju Li,² and Sidney Yip^{3,*}

¹*Department of Mechanical Engineering, Massachusetts Institute of Technology, Cambridge, Massachusetts 02139, USA*

²*Department of Materials Science and Engineering, The Ohio State University, Columbus, Ohio 43210, USA*

³*Departments of Nuclear Engineering and Materials Science and Engineering, Massachusetts Institute of Technology, Cambridge, Massachusetts 02139, USA*

(Received 23 February 2004; published 9 July 2004)

We report the first atomistic calculation of the saddle-point configuration and activation energy for the nucleation of a 3D dislocation loop from a stressed crack tip in single crystal Cu. The transition state is found using reaction pathway sampling schemes, the nudged elastic band, and dimer methods. For the (111)[$\bar{1}10$] crack, loaded typically at 75% of the athermal critical strain energy release rate for spontaneous dislocation nucleation, the calculated activation energy is 1.1 eV, significantly higher than the continuum estimate. Implications concerning homogeneous dislocation nucleation in the presence of a crack-tip stress field are discussed.

DOI: 10.1103/PhysRevLett.93.025503

PACS numbers: 61.72.-y, 62.20.-x, 82.20.Pm

A central issue in understanding the ductile versus brittle behavior of solids is the local response of an atomically sharp crack at critical loading [1–5]. While it is widely recognized that cleavage decohesion and dislocation emission are the two major competing modes of response, atomistically accurate analysis of dislocation loop emission in the presence of a crack-tip stress field has not been carried out. In this Letter we perform reaction pathway analysis using a many-body interatomic potential to determine the atomic configurations that make up the activated displacement fields (shear and tensile) surrounding a crack tip under prescribed load, and the associated energetics. In this way we obtain, in full atomistic details, a description of the emission of an embryonic dislocation loop from the crack tip. Comparing our findings with existing continuum-level treatments, we show that inclusion of atomic-level details gives rise to quantitative corrections which are physically understandable. The implication of our results is that homogeneous nucleation [6] of a dislocation loop at an atomically smooth crack tip in a ductile crystal like Cu is unlikely to be a dominant process. It also follows that local structural heterogeneities, such as a crack-tip ledge, are likely to govern the brittle-ductile response of a solid, for which an atomic-level description along the lines presented here is now feasible.

From a continuum perspective, crack-tip dislocation emission corresponds to the birth and shedding of a shear-type singularity (the dislocation) from the primary, tensile-type singularity (the crack tip). Atomistically, the embryonic dislocation emerges from the stressed crack tip as a distribution of shear displacements between atoms across the slip plane [7]. As the applied strain energy release rate G increases to the critical value for spontaneous dislocation emission, defined here as the athermal G_{emit} , the incipient shear emanating from the crack tip loses its stability, which leads to a fully formed straight dislocation that moves away from the crack. For loads less

than G_{emit} , dislocation emission can occur by overcoming activation energy barriers via thermal fluctuations. This is a very localized process involving the unstable emission of a 3D dislocation loop from a crack tip [3]. Based on the Peierls concept [8], the saddle-point configurations and the associated activation energies have been calculated by recourse to the interplanar potential (γ surface) and approximate numerical schemes of finding unstable transition states [6,9–11]. Although these continuum models provide great physical insights into the nucleation events, a complete understanding of the thermally activated process of dislocation nucleation necessitates a fully atomistic study of the emission of a 3D dislocation loop from a crack tip.

Consider a semi-infinite crack in an otherwise perfect fcc single crystal Cu, schematically shown in Fig. 1. The straight crack front, lying on a (111) plane, runs along the [$\bar{1}10$] direction. The activated slip plane under mode I loading is ($\bar{1}\bar{1}1$), inclined at $\theta = 70.53^\circ$ with respect to the (111) crack plane. Our simulation cell consists of a cracked cylinder cut from the crack tip, with radius $R = 80 \text{ \AA}$. The atoms within 5 \AA of the outer surface are fixed according to a prescribed boundary condition, while all remaining atoms are free to move. To capture the 3D

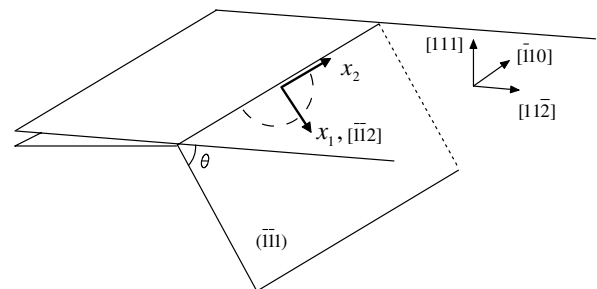


FIG. 1. Orientations of the crack and the inclined ($\bar{1}\bar{1}1$) slip plane across which a dislocation loop nucleates.

nature of a dislocation loop emitted from the crack tip, the simulation cell along the cylinder is taken to be suitably long, i.e., consisting of 24 unit cells with a total length about 61 Å. The periodic boundary condition is imposed along this direction. The effects of finite size on the simulation results will be discussed later. Considering that an atomically sharp crack tip in Cu is unstable and will spontaneously blunt by emitting a dislocation [12], one half layer of atoms is removed to generate a stable, but slightly blunted crack. The total number of atoms within the system is 103 920. The interatomic interactions are modeled using the embedded atom method (EAM) potential of Cu [13]. The unstable stacking energy γ_{us} given by the potential was fitted to the *ab initio* calculation, $\gamma_{us} = 158 \text{ mJ/m}^2$.

Prior to identifying pathways of thermally activated dislocation nucleation, we first determine the athermal load G_{emit} , the value at which the activation energy barrier for dislocation nucleation vanishes, leading to an instantaneous emission of a straight dislocation without thermal fluctuations. We apply incrementally a mode I load G , or the equivalent stress intensity factor K_I . At each step, the initial positions of atoms are set according to the anisotropic linear elastic Stroh solution [14]. Then the system is relaxed using the conjugate gradient method while the outer boundary is held fixed. As in previous studies [15], at low loads we observed the emergence of an embryonic dislocation in the form of a distribution of shear displacements of atoms across the $(\bar{1}\bar{1}1)$ slip plane in front of the crack tip. This incipient dislocation with a straight core along the crack front is only partially formed in that the maximum shear displacement between two crack-tip atoms across the adjacent $(\bar{1}\bar{1}1)$ slip planes is less than one half the Burgers vector $\mathbf{b} = a_0/6[\bar{1}\bar{1}2]$ of a fully formed Shockley partial dislocation, where $a_0 = 3.615 \text{ Å}$ is the lattice constant of Cu. As the applied load increases to $K_{I\text{emit}} = 0.508 \text{ MPa}\sqrt{\text{m}}$ (or the equivalent $G_{\text{emit}} = 1.629 \text{ J/m}^2$ based on the Stroh solution [14]), the metastable state (local energy-minimum) corresponding to the atomic configuration with a partially formed dislocation disappears from the energy landscape (spinodal instability). At this point a straight $a_0/6[\bar{1}\bar{1}2](\bar{1}\bar{1}1)$ Shockley partial dislocation is emitted from the crack tip. The leading edge of the newly formed dislocation moves away from the crack and stops against the fixed outer boundary at about 40 Å from the crack tip, laying down a stacking fault in its wake. As both the crack front and outer boundary of the simulation cell are translationally invariant with respect to the x_2 direction, the final energy-minimized state also possesses a straight dislocation parallel to x_2 axis. We note that the athermal G_{emit} from the present atomistic calculation is higher than the value given by the analytic criterion [4], i.e., $G_{\text{emit}} = 8\gamma_{us}/[(1 + \cos\theta)\sin^2\theta] = 1.067 \text{ J/m}^2$, as the latter was derived without considering the resistance to crack-front surface production in association with dislocation emission [11,12,16].

For a given load below G_{emit} , we use the nudged elastic band (NEB) method [17] to determine the minimum-energy path (MEP) [17] of a partial dislocation loop bowing out from the initially straight crack front. In configurational space, the state with the highest energy along the MEP is the saddle point on the edge of the energy basin enclosing the initial state. For each NEB calculation at a given G , we obtain the initial state by first taking the atomic configuration set according to the linear Stroh solution and then relaxing it by energy minimization. It follows that a partially formed embryonic dislocation with a straight core emerges and remains stable near the crack tip. In contrast, the final state contains a fully formed Shockley partial dislocation, which is also straight. This state is achieved by unloading the simulation cell containing a preexisting Shockley partial dislocation generated by loading the system above G_{emit} . Then a discretized path consisting of 15 replicas of the system is constructed to connect the initial and final states. To allow for nucleation of a curved dislocation, we choose intermediate replicas containing embryonic loops which can emerge from the relaxation of a straight crack front loaded above G_{emit} . The calculation is considered converged when the potential force on each replica vertical to the path is less than 0.005 eV/Å . Based on the result of NEB relaxation, we use the dimer method [18] to refine the calculations of both the saddle-point configuration and the associated activation energy ΔE_{act} . The latter is defined as the energy difference between the saddle point and initial state. The replica with the highest energy from a converged NEB relaxation is taken as the initial input to the dimer method. For the final relaxed dimer, we find the local curvature of energy surface along the dimer direction to be negative and the potential forces on two images in the direction of the dimer are 0.003 and -0.003 eV/Å , respectively, the opposite sign indicating the two images are sitting on two sides of the saddle point.

The MEP of a dislocation loop bowing out at a typical load $G = 0.75G_{\text{emit}}$ is shown in Fig. 2. With the initial-state energy as a reference, the energy variation ΔE along the MEP can be seen. The normalized reaction coordinate is defined as the ratio between l , the hyperspace arc length along the MEP from the initial to the current state, and l_0 , the total arc length along the MEP. The continuous energy curve is obtained by cubic-polynomial interpolation of the calculated energies of replicas, indicated by circles, with the aid of the potential force projected in the direction of the path on each replica [19]. The activation energy ΔE_{act} from the refined calculation using the dimer method is 1.1 eV . For comparison the MEP of nucleating a straight dislocation in the present simulation cell is also shown. Note that the activation energy of nucleating a straight dislocation is known to diverge with increasing length of crack front [9–11]. However, for the present calculation with a finite size of simulation cell, the process of emitting a straight dislocation represents a competing nucleation mechanism for

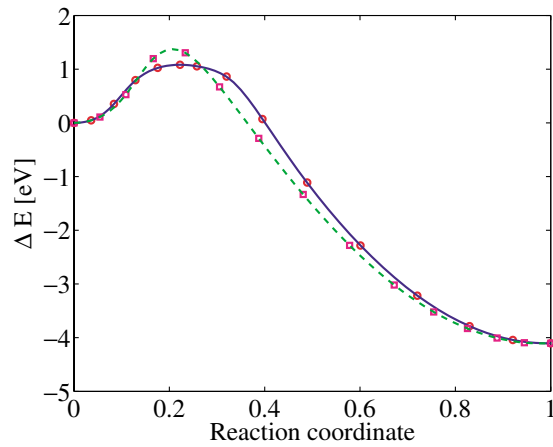


FIG. 2 (color online). The minimum energy paths for nucleating a dislocation loop (solid line) and a straight dislocation (dashed line).

the same set of initial and final states. As the length of simulation cell along the x_2 direction has already been taken to be sufficiently long, it is seen that the activation energy barrier ΔE_{act} for nucleating a 3D dislocation loop is lower than that for a straight dislocation. The difference in ΔE_{act} from the refined calculations using the dimer method is about 0.31 eV.

Along the MEP of nucleating a 3D dislocation loop, dislocation emission is seen as a localized outward protrusion from the straight crack front [20]. This incipient bulge expands subsequently by spreading out in both the forward and lateral directions. The atomic structure of the saddle-point configuration obtained from the dimer method is shown in Fig. 3(a), where all the perfectly coordinated atoms are removed for clarity, and the remaining atoms are those in the core of the protruding dislocation loop, along with those on the crack surfaces. Figure 3(b) shows the distribution of shear displacement in the x_1 direction across two adjacent $(\bar{1}\bar{1}1)$ slip planes containing the dislocation loop shown in Fig. 3(a). The continuous distribution is obtained by cubic-spline interpolation of the normalized shear displacements at discrete lattice sites. It is evident from Fig. 3(b) that the embryonic dislocation develops in the form a nonuniform distribution of shear displacement across the slip plane. The maximum slip occurs right at the crack front with a value of $1.13b$, while minimum slip along the crack front is $0.41b$. The contour line of $b/2$ shear displacement (in green) represents approximately the locus of dislocation core as shown in Fig. 3(a). Within the region enclosed by the dislocation loop, slips between pairs of atoms across the slip plane are around one b , indicating this part of the crack tip has been swept by a fully formed dislocation. In contrast, for pairs of atoms outside the loop, the slips are less than $b/2$. Additionally, Fig. 3(a) shows that the coordination numbers of two rows of crack-front atoms within the end points of the loop change from values of 9 and 12 at the initial state to 10 and 11 at the transition

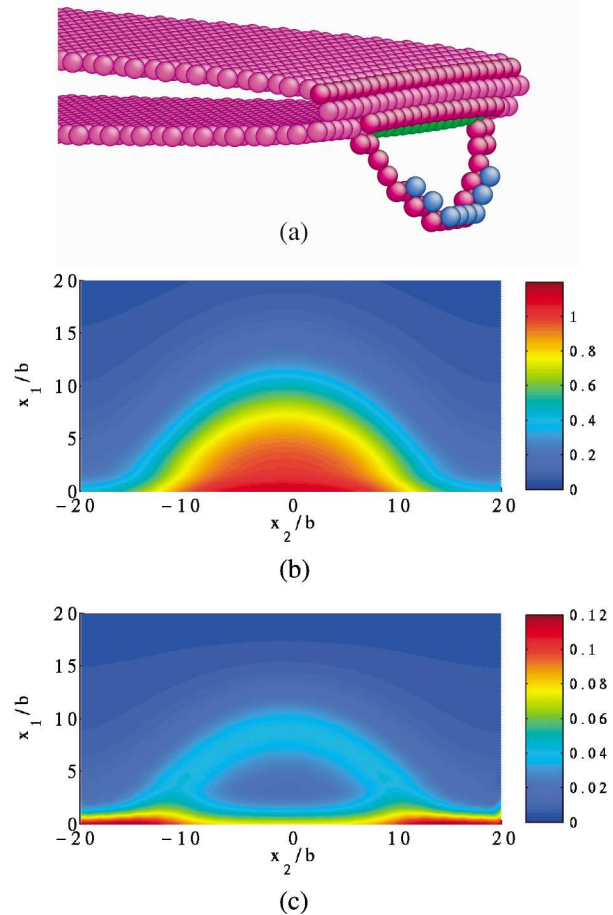


FIG. 3 (color). The saddle-point configuration at $G = 0.75G_{\text{emit}}$ under mode-I load. (a) Atomic structure of dislocation loop. Atom color indicates coordination number N : light pink, $N = 9$, green, $N = 10$, dark pink, $N = 11$, blue, $N = 13$, atoms with perfect coordination $N = 12$ are made invisible; (b) contour plot of shear displacement distribution, normalized by $b = a_0/\sqrt{6} = 1.476 \text{ \AA}$, across the slip plane; (c) contour plot of opening displacement distribution, normalized by the interplanar spacing $h_0 = a_0/\sqrt{3} = 2.087 \text{ \AA}$.

state, respectively, signifying crack-front surface production [11,12,16].

The normal displacement across the slip plane is also of interest since a larger opening has the effect of reducing the resistance for dislocation nucleation [11]. Figure 3(c) shows the corresponding distribution of normalized opening displacement between the same pair of adjacent $(\bar{1}\bar{1}1)$ planes. The maximum opening also occurs at the crack front with a value of $0.12h_0$. A ring of relatively large opening displacements (in light blue) develops ahead of the crack, corresponding to the loop shown in Figs. 3(a) and 3(b). This is the locus of the dislocation core where large shear-induced dilations exist across the slip plane.

Further comparison of the present atomistic results relative to continuum-level findings [10,11] shows quantitative differences in the contour of the saddle point configuration and the magnitude of the activation energy.

One should keep in mind, however, that besides differences in the methods used and the way constitutive behavior are specified, the previous studies were concerned with mode II loading where the activated slip is along the crack plane and the effects of shear-tension coupling and surface-production resistance are known to be weak. Figure 3(b) indicates that, at the saddle-point state, the dislocation has extended in the forward direction by about $10b$ and spreaded out along the crack front by about $30b$. Previous results on the saddle-point loop configuration [10,11] showed forward and lateral extensions of less than $5b$ and $20b$, respectively. For the activation energy ΔE_{act} , the present result of 1.1 eV is significantly larger than a first continuum estimate, based on a perturbative approach, of 0.18 eV [10] and a second, improved estimate of 0.41 eV using a more flexible representation of the incipient dislocation loop [11]. It is physically reasonable that the atomistic treatment should give a higher value than a continuum description since the former is presumably capable of capturing more fully the effects of surface production on the atomic level.

The activation energy allows one to estimate the rate of thermally activated dislocation nucleation. Nucleation from a straight crack front, commonly referred to as homogeneous nucleation [6], should be distinguished from nucleation from discrete heterogeneities along the crack front, such as a ledge, where local crack-front reorientation facilitates nucleation of a screw dislocation, involving no significant surface production and therefore lower thermal activation barrier [6,21]. For the present problem of homogenous nucleation, the frequency of nucleation events per unit distance along the crack front can be estimated from $\nu = n(c_{\text{shear}}/b) \exp(-\Delta E_{\text{act}}/k_B T)$ [10], where $c_{\text{shear}} = 3 \text{ km/s}$ is the shear wave speed, and $n = 1/30b$ is the number of nucleation sites per unit length of crack front. Here, $30b$ is taken in light of the range that the loop spreads out along the crack front laterally. Then one finds $\nu \approx 1.0/(\text{s}\cdot\text{mm})$ at room temperature. Taking $\nu \approx 10^6/(\text{s}\cdot\text{mm})$ to be the threshold for thermally activated nucleation in metal in laboratory measurements [10], we conclude that experimental observation of homogeneous nucleation is unlikely. On the other hand, the presence of any heterogeneity along the crack front can significantly reduce the activation energy for a local process [6,21]. For any specified heterogeneity, the atomistic method presented in this work should be applicable.

We conclude by commenting on the size effect of our simulation cell. It has been shown that attraction between neighboring loops, due to periodicity along the crack front, leads to an underestimate of ΔE_{act} , and a period of $32b$ is sufficient to obtain an accurate value for the activation energy of an isolated loop [11]. Our choice of simulation cell with a period of about $40b$ is based on this result. Regarding the effect of inplane radius R of the cell, we have seen in Fig. 3 that the dislocation loop at the

saddle-point configuration is localized near the crack tip. Hence, the effect of cell boundary on the transition state is expected to be much weaker than that on the final state, where the equilibrium location of a fully formed dislocation sensitively depends on the size of the simulation cell. We have studied finite-size effects in the nucleation of straight dislocation which is computationally less demanding. The 2D nature of the problem requires only a thickness of about 10 \AA along the crack front following the minimum-image convention. Comparing the values of ΔE_{act} for $R = 80 \text{ \AA}$ and 120 \AA [20], we find the difference is less than 6%. We therefore believe that size effects should not affect the accuracy of the saddle-point configuration and the activation energy reported here.

T. Z. and S. Y. acknowledge support by NSF, Honda R&D, DARPA-ONR, and the Lawrence Livermore National Laboratory. J. L. acknowledges support by Honda R&D Co., Ltd. and the OSU Transportation Research Endowment Program.

*Electronic address: syip@mit.edu

- [1] R. W. Armstrong, *Mater. Sci. Eng.* **1**, 251 (1966).
- [2] A. Kelly, W. R. Tyson, and A. H. Cottrell, *Philos. Mag.* **15**, 567 (1967).
- [3] J. R. Rice, and R. Thomson, *Philos. Mag.* **29**, 73 (1974).
- [4] J. R. Rice, *J. Mech. Phys. Solids* **40**, 239 (1992).
- [5] N. Bernstein, and D. W. Hess, *Phys. Rev. Lett.* **91**, 025501 (2003).
- [6] G. Xu, A. S. Argon, and M. Ortiz, *Philos. Mag. A* **75**, 341 (1997).
- [7] A. S. Argon, *Acta Metall.* **35**, 185 (1987).
- [8] R. Peierls, *Proc. Phys. Soc. London* **52**, 34 (1940).
- [9] G. Schoeck, and W. Püschl, *Philos. Mag. A* **64**, 931 (1991).
- [10] J. R. Rice and G. E. Beltz, *J. Mech. Phys. Solids* **42**, 333 (1994).
- [11] G. Xu, A. S. Argon, and M. Ortiz, *Philos. Mag. A* **72**, 415 (1995).
- [12] J. Schiotz, and A. E. Carlsson, *Philos. Mag. A* **80**, 69 (2000).
- [13] Y. Mishin *et al.*, *Phys. Rev. B* **63**, 224106 (2001).
- [14] A. N. Stroh, *Philos. Mag.* **7**, 625 (1958).
- [15] F. Cleri, S. Yip, D. Wolf, and S. R. Phillpot, *Phys. Rev. Lett.* **79**, 1309 (1997).
- [16] S. J. Zhou, A. E. Carlsson, and R. Thomson, *Phys. Rev. Lett.* **72**, 852 (1994).
- [17] H. Jónsson, G. Mills, and K. W. Jacobsen, in *Classical and Quantum Dynamics in Condensed Phase Simulations*, edited by B. J. Berne, G. Ciccotti, and D. F. Coker (World Scientific, Singapore, 1998), p. 385.
- [18] G. Henkelman and H. Jónsson, *J. Chem. Phys.* **111**, 7010 (1999).
- [19] G. Henkelman, and H. Jónsson, *J. Chem. Phys.* **113**, 9978 (2000).
- [20] Supplementary information is on the website of <http://alum.mit.edu/www/zhut/prl04/crack.pdf>
- [21] S. J. Zhou and R. Thomson, *J. Mater. Res.* **6**, 639 (1991).